iScience

CellPress
OPEN ACCESS

Article

Renewable-to-ammonia: Configuration strategy and technoeconomic analysis

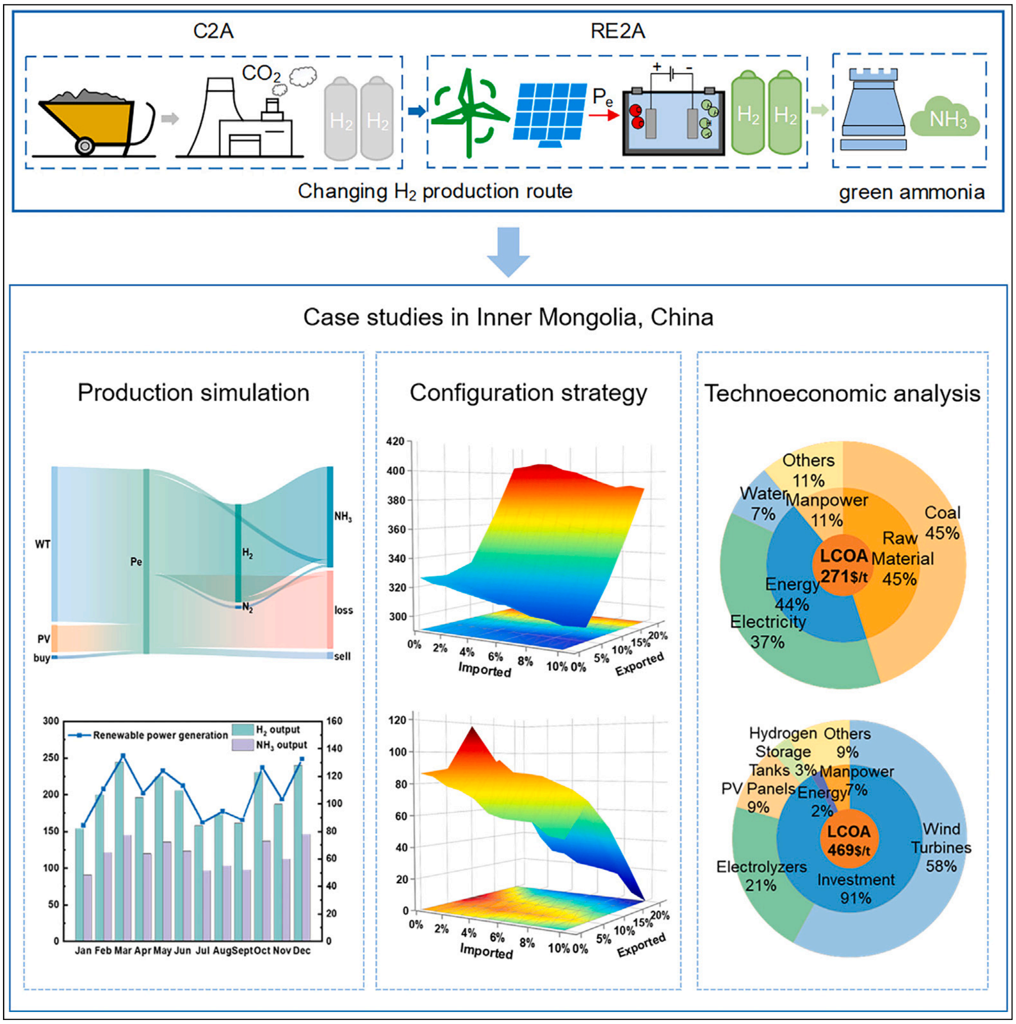

Li Pan, Jiarong Li, Jingsi Huang, ..., Gengyin Li, Ming Zhou, Jianxiao Wang

wang-jx@pku.edu.cn

Highlights

Coal-based ammonia industry is examined to be retrofitted into RE2A via green hydrogen

An optimal configuration strategy is proposed to determine the economic capacity of RE2A

The LCOA is quantified using real-world cases in a RE2A project in Inner Mongolia, China

RE2A performs economic advantages and promising market prospects toward carbon neutrality

Pan et al., iScience *26*, 108512
December 15, 2023 © 2023 The Authors.
https://doi.org/10.1016/j.isci.2023.108512

iScience
CellPress OPEN ACCESS

Article

Renewable-to-ammonia: Configuration strategy and technoeconomic analysis

Li Pan,[1,7] Jiarong Li,[2,3,7] Jingsi Huang,[4] Qi An,[1] Jin Lin,[2] Asad Mujeeb,[2] Yanhui Xu,[1] Gengyin Li,[1] Ming Zhou,[1] and Jianxiao Wang[5,6,8,*]

SUMMARY

The increasing demand for chemical raw materials has provided opportunities for the ammonia (NH_3) industry. However, little attention has been devoted to the economic feasibility of renewable-to-ammonia (RE2A). Therefore, this paper proposes a technoeconomic model to research the optimal capacity configuration and quantify the levelized cost of ammonia (LCOA) for RE2A, which is a retrofitted plant based on coal-to-ammonia (C2A). A cost model of C2A is established as a benchmark to evaluate the economic feasibility of RE2A. A case study in Inner Mongolia is adopted, which shows that the monthly NH_3 output is 7–11$\times 10^3$t, which satisfies actual industrial production. The LCOA of RE2A is 469$/t, with investment in wind turbines accounting for 58%, which is lower than the NH_3 market price (605$–650$/t). The LCOA of RE2A will equal that of C2A with a carbon tax of 47.1$/t CO_2, which confirms the economic advantages of RE2A in the future.

INTRODUCTION

In recent decades, the rapid growth of renewable energy has provided an opportunity for the transition to clean energy in the chemical industry, which will decarbonize traditional chemical manufacturing and expand the utilization of renewable energy in diverse industries.[1–4] On the other hand, converting renewable power to storable and transportable fuels, such as hydrogen (H_2) or H_2 compounds, is a promising solution to address the volatility and mismatched distribution of renewable energy resources.[5–8] Therefore, taking advantage of renewable energy to find an appropriate route that combines environmental and economic advantages for the chemical industry has attracted much attention in both academia and industry.

Given that the technical and economical bottlenecks of H_2 storage and transportation lower the competitiveness of hydrogen energy,[9–11] H_2 carriers, such as ammonia (NH_3), methane, or formic acid, would be a more economical option.[12] Compared with other energy carriers, NH_3 not only is a zero-carbon H_2 carrier[13] but can also be continuously stored and utilized downstream.[14,15] It is commonly used in the manufacturing of nitrogen fertilizers, cryogens, and other organic compounds. Moreover, it is worth mentioning that the growth of conventional H_2-based chemical industries, particularly the NH_3 sector, which is responsible for 15–20% of total chemical sector emissions and 1% of global greenhouse gas emissions,[16,17] has been hampered by both high fossil fuel usage and carbon emissions.[18–20] In 2019, the H_2 consumption to produce NH_3 in China was approximately 10.8 Mt, accounting for 32.3% of the total H_2 demand, which represents the largest H_2 downstream market.[21] Thus, converting renewable power into NH_3 not only aids in the reduction of carbon emissions but also significantly lowers the cost of H_2 storage and transportation. In fact, many countries have put this idea into action, with renewable-to-ammonia (RE2A) demonstration projects in Japan[22] and Australia.[23] China has also issued a related notice on the transformation of synthetic ammonia industrial parks through renewable power supply.[24]

In this context, much work thus far has focused on mathematical modeling and capacity planning for RE2A. A mathematical process model of the NH_3-based energy storage system was introduced[25] and investigated the time-invariant performance. Giovanni Cinti et al. analyzed the power consumption of a solid oxide electrolyzer coupled with a green NH_3 production plant, obtaining a power consumption of 8.3 kWh/kg NH_3 and a system efficiency of 62%.[26] D. Frattini et al. compared the efficiency, energy flows, and carbon emissions of NH_3 synthesis with three different methods of H_2 production, including water electrolysis from renewable energy, biomass gasification and biogas reforming.[27] Hui Du et al. proposed an NH_3-based distributed energy system and compared the carbon emissions of brown and green ammonia, verifying that green ammonia will be more competitive in the future.[28] A flexible operation strategy was proposed for ammonia synthesis using variable

[1]State Key Lab of Alternate Electrical Power System with Renewable Energy Sources, North China Electric Power University, Beijing 102206, China
[2]Department of Electrical Engineering, Tsinghua University, Beijing 100084, China
[3]Harvard John A. Paulson School of Engineering and Applied Sciences, Cambridge, MA 02138, USA
[4]Department of Industrial Engineering and Management, College of Engineering, Peking University, Beijing 100871, China
[5]National Engineering Laboratory for Big Data Analysis and Applications, Peking University, Beijing 100871, China
[6]Peking University Ordos Research Institute of Energy, Ordos 017000, China
[7]These authors contributed equally
[8]Lead contact
*Correspondence: wang-jx@pku.edu.cn
https://doi.org/10.1016/j.isci.2023.108512

Table 1. Optimal configuration strategy of facilities

Facilities	Capacity
wind turbines (MW)	340
photovoltaic panels (MW)	85
electrolyzers (MW)	275
hydrogen storage tanks (10^3 Nm^3)	550

wind and solar energy.[29] The results confirmed that the hybridization of wind and solar can significantly reduce the cost of H_2 and NH_3 production. An optimal combined capacity planning approach for RE2A was proposed.[30] It quantified the levelized cost of energy of the system, yielding a specific result of 0.17$–0.28$/kWh. A global green ammonia network was developed to research the impact of different scales on NH_3 production and transport.[31] An exergoeconomic analysis and optimization of combined wind and solar energy for producing electricity, H_2 and NH_3 were proposed.[32] The study analyzed the impacts of different wind speeds and solar radiation on energy efficiency. The water electrolysis and ammonia synthesis processes were described in detail.[33] The study analyzed the costs of producing ammonia using various types of renewable energy and reactor cooling technologies. Hanxin Zhao et al. established a hybrid optimal simulation model to evaluate the possibility of commercializing green NH_3 in some regions where renewable electricity is in surplus.[34] Co-planning of a wind resource-based ammonia industry and an electric network was proposed, and the results confirmed that the siting and sizing of NH_3 plants are strongly related to wind resources, NH_3 demand, facility costs, and energy transport modes.[35] D. Xu et al. proposed an integrated power-to-NH_3 system incorporating the operational and commuted lifetime deterioration of the nitrogen generator and electrolyzer, which enabled a quantitative economic analysis for a highly renewable multienergy system.[36] Furthermore, different renewable energies have been coupled with NH_3 and investigated in process simulations and feasibility analysis for industrial application.[37,38]

Existing research efforts have been devoted to operation control and capacity configuration strategies of RE2A, providing a mature optimization approach for further studies, yet few examples have focused on the economic feasibility, namely, the technoeconomic analysis of RE2A. To fill this gap, this paper is the first attempt to quantify the levelized cost of ammonia (LCOA) produced from 100% renewable energy. In addition, we evaluate the competitiveness of the LCOA of RE2A compared with that of coal-to-ammonia (C2A) based on the resource endowment (utilization hours and intensity) and initial investment of wind and solar power in a specific region. The major contributions of this paper are as follows.

(1) We change the route of H_2 production to retrofit C2A into RE2A, which produces zero-carbon hydrogen from the coupling of wind and solar power. Based on the system, an optimization model is established to research the optimal capacities of wind turbines, photovoltaic panels, electrolyzers, and hydrogen buffer tanks.
(2) This paper compares the LCOA of C2A and RE2A considering the implementation of a carbon tax ranging from 10$/t$CO_2$ to 60$/t$CO_2$ in China; the results confirm that RE2A is economically feasible and has great potential to achieve industrial application in the future.
(3) Sensitivity analysis of RE2A reveals that investment in wind turbines should be given high priority due to rich wind resources, while the capacity of photovoltaic (PV) panels should be flexible to ensure an appropriate utilization rate of wind turbines, which provides useful guidelines for converting existing C2A to RE2A in Inner Mongolia.

RESULTS AND DISCUSSION

Using the C2A and RE2A system model proposed in STAR methods, an industrial park with an annual output of 1.00×10^5 t of NH_3 is simulated. We analyze the costs of two approaches to meet market demand: C2A and RE2A. The wind and solar data come from Inner Mongolia Province in China, as depicted in Figure S3. The techno-economic parameters of the facilities are listed in Table S1.[39–42] The electricity price used in this section is collected from Inner Mongolia Power (Group) Co., Ltd.[43] It should be noted that the on-grid price of wind and solar power is 40.35$/MWh, while the peak-valley electricity prices are used for industrial customers according to the available renewable resources. We have chosen an alkaline electrolyzer and 30 bar storage tanks because of their mature technologies.[44] It is worth mentioning that vapor is a by-product of the process and can be reused. Therefore, the cost of vapor is ignored in this paper. In this section, we give the optimal configuration strategy of the RE2A facilities. On this basis, the ammonia production cost and carbon tax of the C2A and RE2A systems are used to compare economic performance.

Optimal configuration strategy

To meet the ammonia output of existing industrial parks, a reasonable configuration strategy is required for the RE2A system. This subsection provides the optimal capacity for each facility.

The optimal configuration is obtained by using the proposed model, as shown in Table 1. According to the RE2A demonstration projects released by the Energy Bureau of Inner Mongolia,[45] it invests in wind power with a capacity of 400 MW and in PV power with a capacity of 200 MW in Alashan, with an annual production of 2.23×10^4 t of H_2 and 1.40×10^5 t of NH_3. The scale of this plant is comparable to the configuration strategy we proposed, which justifies that the RE2A system can be implemented in the real world.

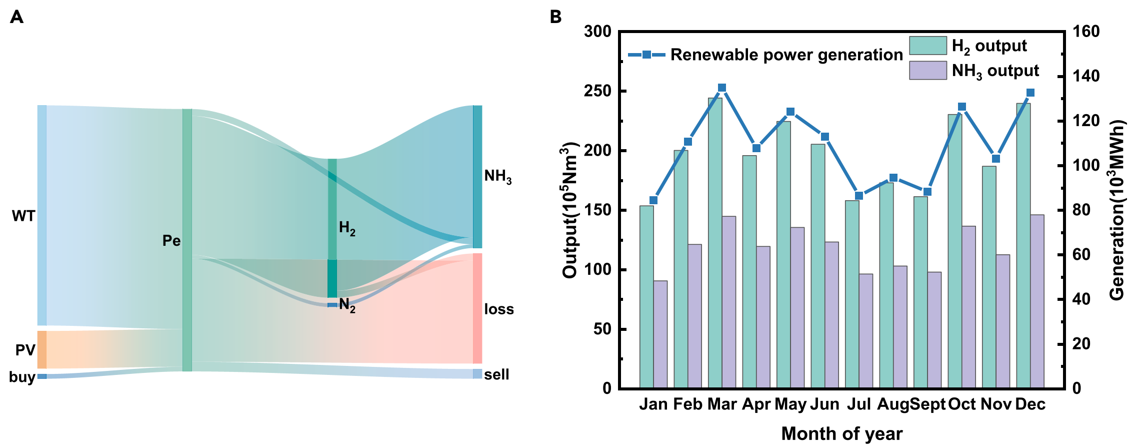

Figure 1. Energy flow and output situation of the RE2A system

(A) Energy flow of the RE2A system.

(B) Monthly H_2 and NH_3 output and renewable power generation.

From the perspective of the whole process, the energy flow of the RE2A system, monthly H_2 and NH_3 output and amount of renewable power generated are depicted in Figure 1.

As seen from the aforementioned results, the optimal capacity of wind power is 340 MW, almost 3 times higher than that of PV, which accounts for 85% of renewable energy power generation. H_2 and NH_3 production is largely determined by the generation of renewable energy. The results are due to Inner Mongolia being one of China's provinces with the most abundant wind resources and with a specific power exceeding 200 W/m^2. This result offers exciting opportunities to convert renewable energy to ammonia. On the other hand, it is observed that approximately 87% of the power flow in the electrolyzers is used to produce H_2, which confirms that electrolysis-based hydrogen production is an appropriate "consumer" for surplus wind and solar power. Due to the 60% conversion efficiency of electricity to hydrogen, nearly half of the energy is lost. Therefore, the H_2 production efficiency of the electrolyzers plays an important role in the entire process. Furthermore, the monthly output is 7–11$\times 10^3$ t NH_3, which satisfies the actual situation of industrial production.

The operation of the proposed approach was evaluated via simulations in four different seasons. Figure 2 displays the operation of electrolyzers and the NH_3 production rate in different seasons, and Figure 3 shows the H_2 inventory in the RE2A system.

In the summer, most interestingly, although there is relatively little electricity to produce H_2, ammonia production is still stable. This may be explained by the hydrogen storage unit, given that the amount of H_2 produced is more than the amount consumed for ammonia synthesis in the sprin and then excess H_2 flows into hydrogen buffer tanks. Thus, there is sufficient H_2 to ensure the stability of ammonia production. In addition, the hydrogen storage unit works as a "cushion" to eliminate hydrogen fluctuations between the electrolyzers and ammonia synthesis reactors, which always operate under steady circumstances with a constant flow rate of the feed gas. Compared to the summer, both hydrogen production and ammonia synthesis are significantly increased in autumn and winter. This increase can be attributed to a superior geographical environment with abundant wind resources.

Economic performance

According to the optimal configuration strategy, the overall investment and operation costs of RE2A can be calculated. On this basis, the levelized cost of ammonia production (LCOP) with investment and LCOA can be obtained to evaluate the economic performance of the RE2A system. The comparison of the LCOPs and LCOAs for C2A and RE2A is shown in Table 2 and Figure 4.

The LCOP for C2A and RE2A is 472$/t and 588$/t, respectively. Considering the existing C2A system, which already has a mature production process, it does not require extra investment. Also, we change the route of H_2 production to retrofit C2A into RE2A, which means only the hydrogen-related components will be invested in RE2A. The asterisk indicates the current ammonia production cost that investors need to spend in C2A and RE2A, namely LCOA. Therefore, the LCOA for C2A includes the costs of coal, energy, and manpower, while that for RE2A includes the investment in H_2 production and the costs of energy and manpower. It should be noted that the subsequent analysis is based on LCOA.

As shown in Figure 4, the cost of raw materials and electricity account for approximately 80% of the LCOA in C2A with investment, while in RE2A, investment in wind turbines and electrolyzers accounts for 58% and 21% of the LCOA, respectively. Furthermore, the LCOA of RE2A is 469$/t, which is lower than the ammonia market price in Inner Mongolia (approximately 605$–650$/t). This result verifies that the green ammonia route is economically feasible. With the decline in facility costs in the long planning horizon, there is great impetus to develop a green ammonia industry chain. In addition, we have quantified the levelized cost of hydrogen (LCOH) of RE2A, 2.11$/kg, which is consistent with existing studies.[46] Meanwhile, the levelized cost of electricity (LCOE) has also been calculated. The LCOE for wind power is 23$/MWh, and for solar power, it is 41$/MWh. These results reveal that the future looks bright for the application of H_2 and NH_3 production via renewable energy in Inner Mongolia.

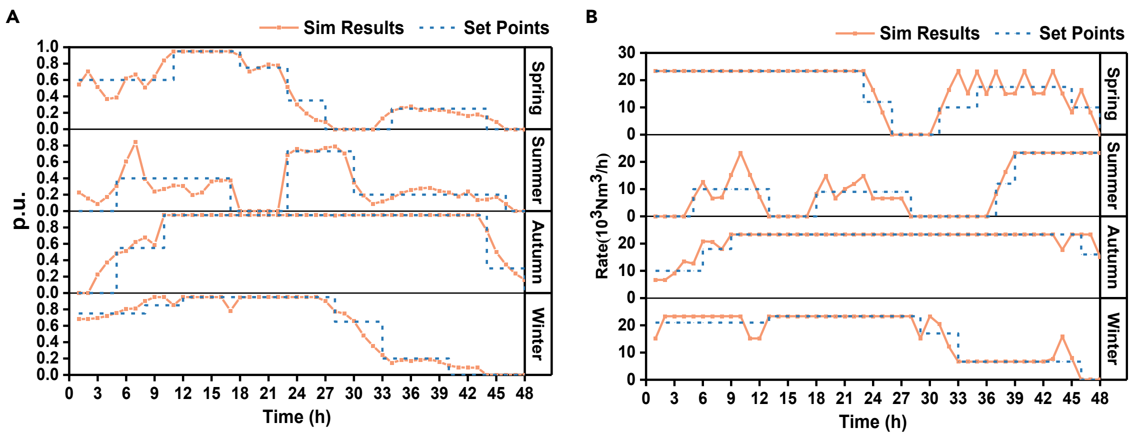

Figure 2. Operation of electrolyzers and NH_3 production rate in different seasons
(A) Operation of electrolyzers.
(B) NH_3 production rate.

It must also be mentioned that C2A always has a high carbon footprint, approximately 4.2 $kgCO_2/kgNH_3$,[47] and has therefore attracted much attention from both the government and academia.[48] Several measures to reduce carbon emissions have also been adopted. Thus, with the implementation of carbon trading in China, the impact of carbon tax on the total production cost (TPC) of the C2A and RE2A system is examined, as shown in Figure 5. As the carbon tax grows from 10\$/t CO_2 to 60\$/t CO_2, the TPC of the C2A system increases remarkably. When it rises to 47.1\$/t CO_2, the TPC of C2A is equal to that of RE2A, and RE2A presents more significant economic benefits as the carbon tax continues to rise. Currently, the carbon market trading price in China is approximately 8.47\$/t CO_2.[49] The shortage of coal resources and the rise in coal prices could result in the restructuring of the energy-consuming industry. Zhang et al. and Hu et al. have predicted that the carbon tax is likely to reach 20\$–35\$/tCO_2 by 2030 in China.[50,51] Also, Lin et al. found that different industries coverage with carbon prices ranging from 10\$ to 57\$/tCO_2 by 2030 led to commodity prices increasing from 0.12 to 1.64%.[52] The price will continue to increase in the future with the further enforcement of carbon reduction policies and popularization of green development, and thus, C2A becomes uneconomic in the case of expensive carbon taxes, which verifies that RE2A is economically feasible and has great potential to achieve industrial application in the future.

Sensitivity analysis

To deeply research the impact of different factors on the costs and configuration strategies of C2A and RE2A, several key parameters are analyzed in this subsection. From the economic performance aforementioned, it can be seen that the LCOA of C2A will be greatly influenced by electricity prices and carbon taxes in the future. Therefore, the electricity price is set in the range of 0.4–1.4 times the current price to

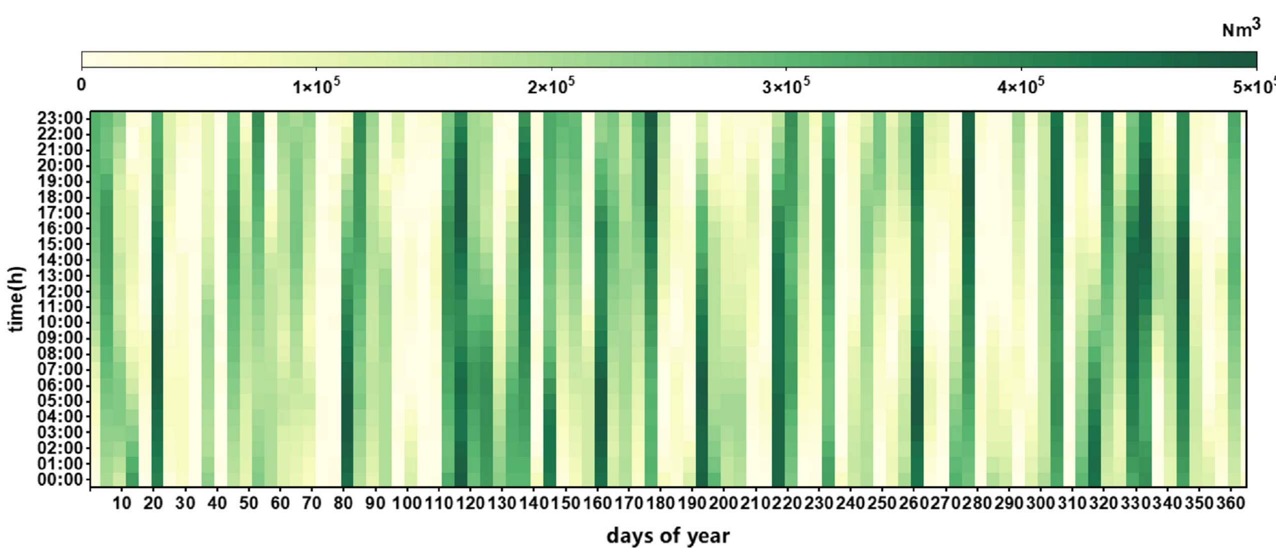

Figure 3. H_2 inventory in the RE2A system.

Table 2. Comparison of the LCOPs for C2A and RE2A

Costs	C2A	RE2A
investment($/t)		
hydrogen production	82	428 *
air separation	25	25
ammonia synthesis	94	94
Coal($/t)	122 *	0
Energy($/t)	119 *	11 *
Manpower($/t)	30 *	30 *
LCOP($/t)	472	588

analyze the LCOA of C2A. The impacts of electricity price and carbon tax on the LCOA of C2A are explored and shown in Figure 6. Obviously, as the carbon tax increases, the LCOA of C2A rises rapidly, even when the electricity price is at the lowest point, and there is no economic advantage compared to RE2A when the carbon tax exceeds 50$/t$CO_2$.

According to Figure 4, the higher cost of RE2A is mostly attributable to the comparatively high investment costs of facilities. To obtain a competitive cost of RE2A, a capital recovery factor (CRF) related to the facilities or the subsidy of facilities in the future is required to establish the RE2A market and provide assistance for substitution of RE2A for C2A. On the other hand, a large amount of power generated from wind and solar flows into the electrolyzers to produce H_2 in the whole process. However, the power consumption of water electrolysis will decrease daily with the maturity of electrochemistry technology.

Therefore, there are three key parameters to be investigated in the RE2A system: CRF, facility subsidies and the efficiency of the electrolyzers. According to Equation 16, it is clear that there are mainly two variables related to CRF: facility lifetime and discount rate. The impacts of lifetime and discount rate on the LCOA of RE2A are shown in Figure 6.

In accordance with expectations, with a gradual decline in CRF, the LCOA also decreases accordingly. Single asterisks in the figure indicate that the LCOA is lower than the market price, while double asterisks indicate that the LCOA for RE2A is lower than that for C2A.

Considering a carbon tax of 20$/t, the LCOA of C2A is only 355$/t. Based on this cost, there are three subsidy types for RE2A to be discussed: (1) Subsidy only for wind turbines. (2) Subsidy only for PV panels. (3) Equal subsidy for wind turbines and PV panels. The performance of different subsidy types is shown in Table 3.

For subsidy types 1 and 2, the LCOA of RE2A can be reduced to 355$/t with a subsidy of 338$/kW for wind turbines, while a subsidy of 419$/kW for PV panels can compensate for the difference, which reveals that wind turbines should be given priority over PV panels in terms of subsidies. Compared with the optimal capacity results, in subsidy type 3, the capacity of wind turbines decreases from 340 MW to 311 MW, whereas that of PV increases from 85 MW to 200 MW. This demonstrates that a less expensive facility must have a higher capacity is necessary to achieve the utilization rate of an expensive facility.

In addition, the impacts of the investment and efficiency of electrolyzers on LCOA and the capacity configuration of RE2A are studied. The results are depicted in Figure 7. The LCOA has a profit margin when the efficiency of the electrolyzers reaches 50% (2.94 kWh/Nm^3 H_2 is the highest efficiency in theory). With the improvement of efficiency, the capacity of wind turbines has a tendency to decrease, while that of PV panels gradually increases, which reveals that lower power consumption is helpful for balancing the capacity of wind and solar power. On the

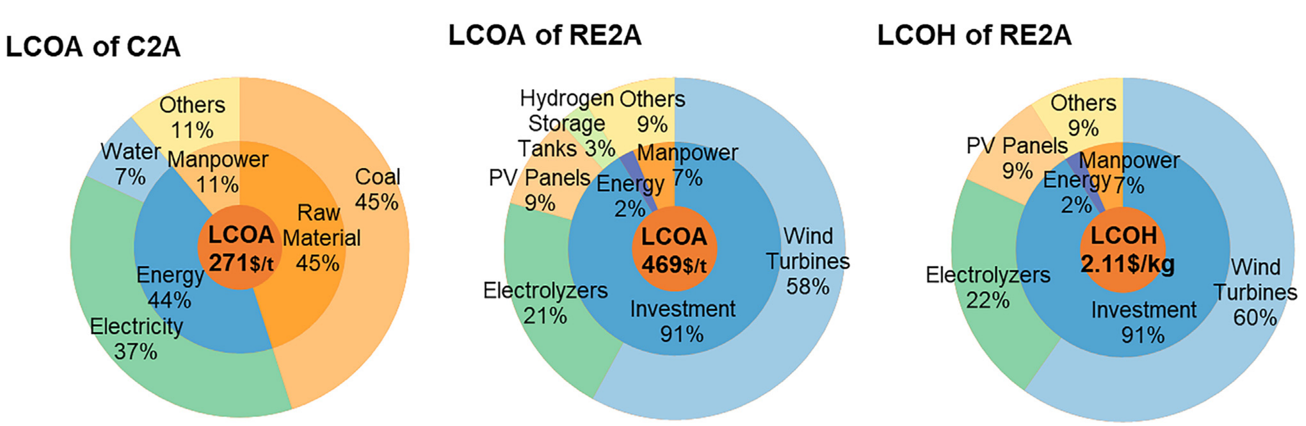

Figure 4. Comparison of the LCOAs for C2A and RE2A.

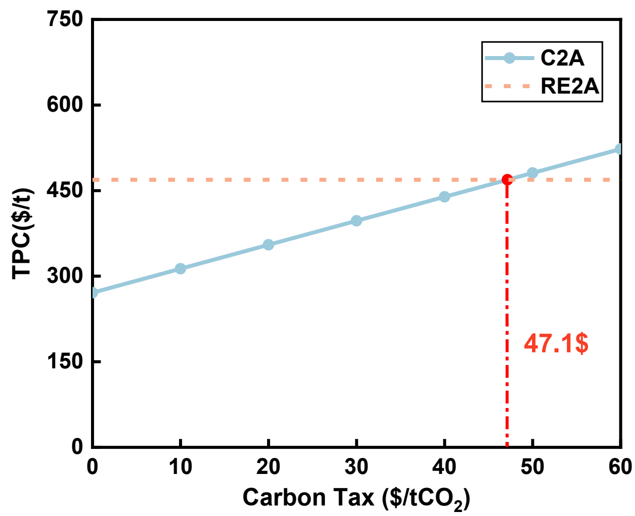

Figure 5. Impact of carbon tax on the TPC of the C2A and RE2A systems.

other hand, the capacity of electrolyzers and hydrogen storage tanks in reduction as efficiency increases, which is one of the reasons for the decrease in LCOA, which is one of the reasons for the decrease in LCOA.

Furthermore, according to the policies implemented in Inner Mongolia, electricity sold to the grid shall not exceed 20% of the total renewable generation capacity for grid-connected projects and shall minimize electricity purchases from the grid as much as possible.[53] Similar to the analysis mentioned previously, the capacity configurations under different ratios of renewable electricity imported and exported to the grid are studied. The results are shown in Figure 8.

As the amount of electricity imported increases, the capacity of wind turbines and PV panels gradually decreases. However, with the growth of exported electricity, the capacity of wind turbines increases correspondingly, while that of PV panels first increases and then decreases as the electricity contribution increases from 0% to 10% and then to 20%. The rate of decline is significantly higher than the rate of increase, which reveals that RE2A should prioritize investment in wind turbines when more power generation is needed.

Conclusions

This paper proposes an optimal capacity configuration of the RE2A system to produce green ammonia. From the perspective of ammonia producers, to substitute the existing route, a new ammonia production route must be profitable and satisfy the market demand. On this basis, a capacity optimization model is proposed to minimize the total investment and operation costs of the RE2A system. Finally, case studies based on data from Inner Mongolia in China are investigated, and conclusions such as the following can be drawn.

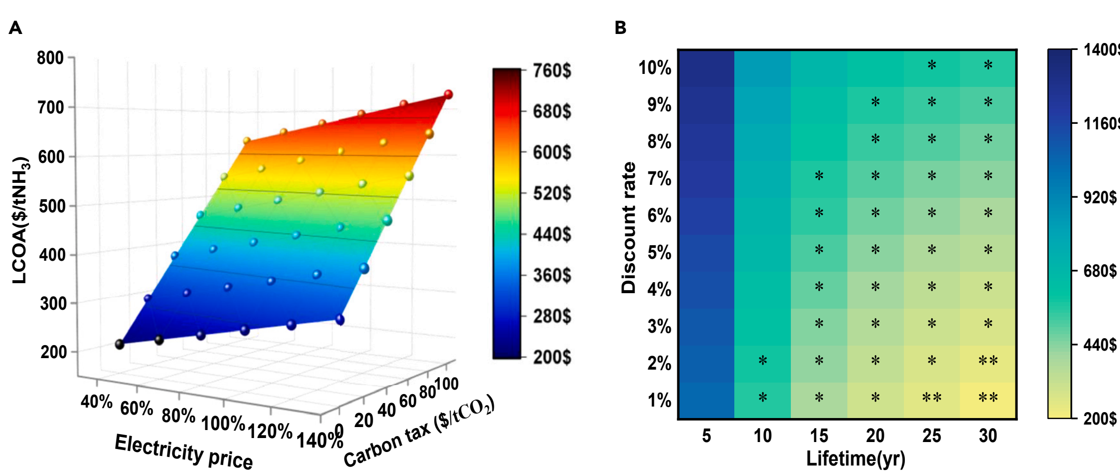

Figure 6. Impacts of key factors on the LCOA of C2A and RE2A

(A) Impacts of electricity price and carbon tax on the LCOA of C2A; (B) impacts of CRF on the LCOA of RE2A.

Table 3. Performance of different subsidy types

Type	Subsidy ($/kW) WP	PV	C^{WP} (MW)	C^{PV} (MW)	C^{EW} (MW)	C^{HS} (10^3 Nm^3)	LCOA ($/t)
1	338	0	404	0	300	767	354.63
2	0	419	75	739	388	328	354.70
3	302	201	311	200	252	320	354.84

(1) The optimal capacity configuration of RE2A not only satisfies the actual situation of industrial ammonia production but also enhances the utilization of renewable energy generation, which verifies the feasibility of RE2A.
(2) The LCOA of RE2A is currently lower than the ammonia market price in China. RE2A will present more significant economic benefits with the implementation of a carbon reduction policy compared to C2A with an extra carbon tax.
(3) CRF, the subsidy of facilities, the efficiency of electrolyzers, and the interactive power are the four key factors related to the LCOA and capacity configuration of RE2A. In particular, investment in wind turbines has a higher priority than investment in PV panels due to the abundant wind resources in Inner Mongolia. The capacity of PV panels is flexible to ensure the utilization rate of wind turbines.

Limitations of the study

Given that the primary purpose of this research is to propose optimal configuration strategies and assess the economic feasibility of RE2A, the scope is limited to LCOA analysis of specific scenarios. In addition, it is important to emphasize that the technoeconomic model presented herein can be improved or expanded to research other strategies for converting renewable energy to chemicals. Therefore, we outline some limitations of the study.

Power supply system: The RE2A system analyzed in this study is driven solely by wind and PV power; no hybrid systems (e.g., combined heat and power or waste heat recovery) or energy storage devices are considered. However, we note that these systems may be more energy efficient and that the additional energy storage ensures a near-constant power supply to the electrolyzers. These systems are excluded from the scope of this study since we have chosen a region with abundant renewable energy for demonstration purposes. It is suggested that future studies incorporate these systems to evaluate LCOA in other general areas.

Impact of different electrolytic cells on LCOA: Within RE2A configurations, only mature electrolytic water technologies with acceptable cost and performance are used in industrial applications. We have chosen an alkaline electrolyzer in this study, while proton exchange membrane electrolytic cells and solid oxide cells will become widely applied in various fields with the development of electrochemistry. Investment in electrolyzers ranks second among TPCs. Thus, it is necessary to research the impacts of different electrolysis cells on the LCOA of RE2A systems in the future.

Impact of resource recovery on LCOA: Throughout the process of NH_3 synthesis, a large number of by-products are generated, which represent extra revenue for the system. This study does not account for resource recovery, such as sulfur from the desulfurization unit and

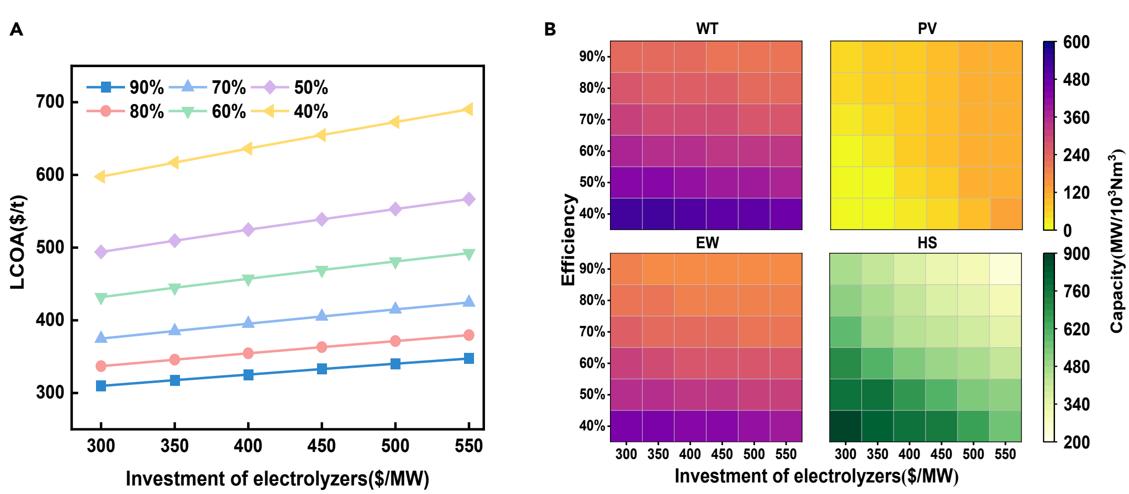

Figure 7. The impacts of investment and efficiency of electrolyzers on LCOA and capacity configuration of RE2A

(A) The impacts of investment and efficiency of electrolyzers on LCOA.

(B) The impacts of the investment and efficiency of electrolyzers on the capacity configuration of RE2A.

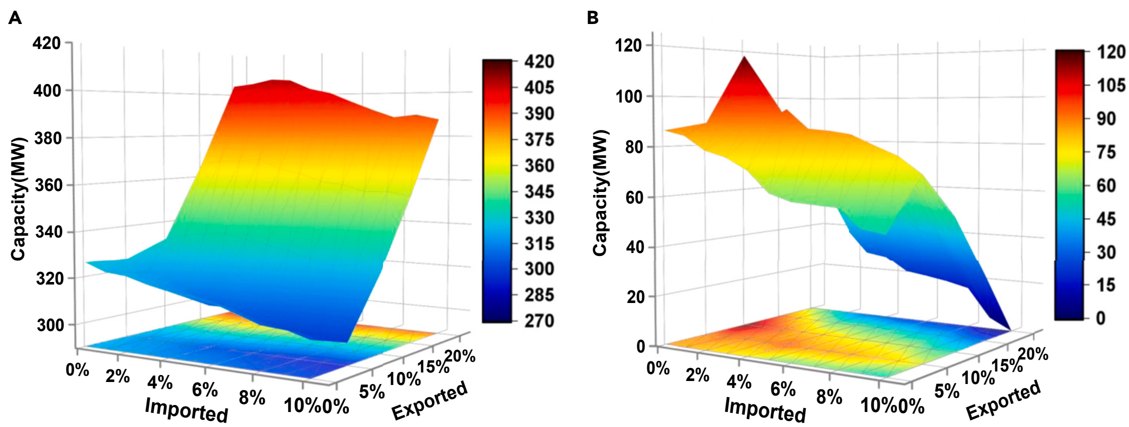

Figure 8. Impact of renewable electricity imported and exported to the grid on the capacity configuration of RE2A

(A) Capacity configuration of wind turbines.

(B) Capacity configuration of photovoltaic panels.

O_2 separated from water. The economic value of these recovered products can offset the system cost to a certain extent. We do not consider it because this study focuses on comparing the LCOA of C2A and RE2A, rather than on obtaining an accurate LCOA. It is advised that prospective studies consider these factors to obtain accurate LCOA estimates.

Acronyms

The acronyms used in this paper are listed in Table 4.

STAR★METHODS

Detailed methods are provided in the online version of this paper and include the following:

- KEY RESOURCES TABLE
- RESOURCE AVAILABILITY
  - Lead contact
  - Materials availability
  - Data and code availability
- METHOD DETAILS
  - Coal-to-ammonia system
  - Renewable-to-ammonia system
  - Data resources

Table 4. List of acronyms

Term	Acronym	Term	Acronym
Ammonia synthesis	AS	Levelized cost of electricity	LCOE
Air Separation Unit	ASU	Levelized cost of hydrogen	LCOH
Capital recovery factor	CRF	Levelized cost of ammonia production	LCOP
Coal-to-ammonia	C2A	Manpower	MP
Coal-to-hydrogen	C2H	Nitrogen separation	NS
Energy consumption	EC	Oxygen separation	OS
Electrolysis of water	EW	Pressure Swing Adsorption	PSA
Expenditure	EX	Photovoltaic	PV
Hydrogen storage	HS	Renewable-to-ammonia	RE2A
Investment	IN	Total production cost	TPC
Levelized cost of ammonia	LCOA	Wind power	WP

SUPPLEMENTAL INFORMATION

Supplemental information can be found online at https://doi.org/10.1016/j.isci.2023.108512.

ACKNOWLEDGMENTS

This work was supported by National Key Research and Development Program of China (No. 2021YFB4000104), National Natural Science Foundation of China (No. 52277092), and State Key Laboratory of Alternate Electrical Power System With Renewable Energy Sources (North China Electric Power University) (No. LAPS22021).

AUTHOR CONTRIBUTIONS

Conceptualization, L. P., J. L., and J. W.; Methodology, L. P., Q. A., and J. W.; Investigation, J. L, J. H., and A. M.; Writing – Original Draft, L. P. and J. L.; Writing – Review & Editing, L. P., J. L., Q. A., and J. W.; Visualization, L. P. and Q. A.; Supervision, J. L., G. L., and M. Z.; Funding acquisition, J. L, Y. X., and J. W.

DECLARATION OF INTERESTS

The authors declare no competing interests.

Received: May 18, 2023
Revised: August 6, 2023
Accepted: November 19, 2023
Published: November 22, 2023

REFERENCES

1. Wang, J., Zhong, H., Yang, Z., Wang, M., Kammen, D.M., Liu, Z., Ma, Z., Xia, Q., and Kang, C. (2020). Exploring the trade-offs between electric heating policy and carbon mitigation in China. Nat. Commun. *11*, 6054.
2. Varone, A., and Ferrari, M. (2015). Power to liquid and power to gas: An option for the German Energiewende. Renew. Sustain. Energy Rev. *45*, 207–218.
3. Yu, Y., Wang, J., Chen, Q., Urpelainen, J., Ding, Q., Liu, S., and Zhang, B. (2023). Decarbonization efforts hindered by China's slow progress on electricity market reforms. Nat. Sustain. *6*, 1006–1015.
4. Wu, Z., Wang, J., Zhou, M., Xia, Q., Tan, C.-W., and Li, G. (2022). Incentivizing frequency provision of power-to-hydrogen toward grid resiliency enhancement. IEEE Trans. Ind. Inf. *19*, 1–10.
5. Guo, H., Huang, L., and Liang, D. (2022). Further promotion of sustainable development goals using science, technology, and innovation. Innovation *3*, 100325.
6. Blanco, H., and Faaij, A. (2018). A review at the role of storage in energy systems with a focus on Power to Gas and long-term storage. Renew. Sustain. Energy Rev. *81*, 1049–1086.
7. Abdin, Z., Tang, C., Liu, Y., and Catchpole, K. (2021). Large-scale stationary hydrogen storage via liquid organic hydro-gen carriers. iScience *24*, 102966.
8. Li, Y., Lan, S., Ryberg, M., Pérez-Ramírez, J., and Wang, X. (2021). A quanti-tative roadmap for China towards carbon neutrality in 2060 using methanol and ammonia as energy carriers. iScience *24*, 102513.
9. Wang, J., Gao, F., Zhou, Y., Guo, Q., Tan, C.-W., Song, J., and Wang, Y. (2023). Data sharing in energy systems. Advances in Applied Energy *10*, 100132.
10. Wang, J., An, Q., Zhao, Y., Pan, G., Song, J., Hu, Q., and Tan, C.-W. (2023). Role of electrolytic hydrogen in smart city decarbonization in China. Appl. Energy *336*, 120699.
11. Wu, Z., Wang, J., Zhong, H., Gao, F., Pu, T., Tan, C.-W., Chen, X., Li, G., Zhao, H., Zhou, M., and Xia, Q. (2022). Sharing economy in local energy markets. J. Modern Power Syst. Clean Energy *11*, 1–13. early access. https://ieeexplore.ieee.org/document/9989335.
12. Yue, M., Lambert, H., Pahon, E., Roche, R., Jemei, S., and Hissel, D. (2021). Hydrogen energy systems: A critical review of technologies, applica-tions, trends and challen-ges. Renew. Sustain. Energy Rev. *146*, 111180.
13. Jain, M., Muthalathu, R., and Wu, X.-Y. (2022). Electrified ammonia production as a commodity and energy storage medium to connect the food, energy, and trade sectors. iScience *25*, 104724.
14. Wang, J., Zhong, H., Ma, Z., Xia, Q., and Kang, C. (2017). Chongqing Kang. Review and prospect of integrated demand response in the multi-energy system. Appl. Energy *202*, 772–782.
15. Yüzbaşıoğlu, A.E., Tatarhan, A.H., and Gezerman, A.O. (2021). Decarboniza-tion in ammonia production, new technological methods in industry-ial scale ammonia production and critical evaluations. Heliyon *7*, e08257.
16. IRENA and AEA (2022). Innovation Outlook: Renewable Ammonia, International Renew-able Energy Agency. Abu Dhabi, Ammonia Energy Association. https://www.irena.org/Publications/2022/May/Innovation-Outlook-Renewable-Ammonia.
17. MacFarlane, D.R., Cherepanov, P.V., Choi, J., Suryanto, B.H.R., Hodgetts, R.Y., Bakker, J.M., Ferrero Vallana, F.M., and Simonov, A.N. (2020). A Roadmap to the ammonia economy. Joule *4*, 1186–1205.
18. Wang, F., Harindintwali, J.D., Yuan, Z., Wang, M., Wang, F., Li, S., Yin, Z., Huang, L., Fu, Y., Li, L., et al. (2021). Technologies and perspectives for achieving carbon neutrality. Innovation *2*, 100180.
19. Chen, J.M. (2021). Carbon neutrality: Toward a sustainable future. Innovation *2*, 100127.
20. Wang, L., Xia, M., Wang, H., Huang, K., Qian, C., Maravelias, C.T., and Ozin, G.A. (2018). Greening ammonia toward the solar ammo-nia refinery. Joule *2*, 1055–1074.
21. China Hydrogen and Fuel Cell Industry Handbook (2020, China hydrogen alliance. http://h2cn.org.cn/dynamics.html.
22. CO_2-Free Ammonia Synthesis - CO_2-Free Energy Carrier (2019). https://www.jgc.com/en/business/techinnovation/environment/co2-free.html.
23. Ammonia Plant Revamp to Decarbonize: Yara Pilbara (2019. https://ammoniaindustry.com/ammonia-plant-revamp-to-decarbonize-yara-pilbara/.
24. Inner Mongolia Autonomous Region Energy Bureau (2023). Notice of the Energy Bureau of Inner Mongolia Autonomous Region on the issuance of the list of green power supply projects in the second batch of industrial parks. https://nyj.nmg.gov.cn/zwgk/zfxxgkzl/fdzdgknr/tzgg_16482/tz_16483/202301/t20230105_2197915.html.
25. Wang, G., Mitsos, A., and Marquardt, W. (2017). Conceptual design of ammonia-based energy storage system: System design and time-invariant performance. AIChE J. *63*, 1620–1637.
26. Cinti, G., Frattini, D., Jannelli, E., Desideri, U., and Bidini, G. (2017). Coupling Solid Oxide Electrolyser (SOE) and ammonia production plant. Appl. Energy *192*, 466–476.
27. Frattini, D., Cinti, G., Bidini, G., Desideri, U., Cioffi, R., and Jannelli, E. (2016). A system approach in energy evaluation of different renewable energies sources integration in ammonia production plants. Renew. Energy *99*, 472–482.
28. Du, H., Shen, P., Chai, W.S., Nie, D., Shan, C., and Zhou, L. (2022). Perspective and analysis of ammonia-based distributed energy system

(DES) for achiev-ing low carbon community in China. iScience *25*, 105120.
29. Armijo, J., and Philibert, C. (2020). Flexible production of green hydrogen and ammonia from variable solar and wind energy: Case study of Chile and Argentina. Int. J. Hydrogen Energy *45*, 1541–1558.
30. Palys, M.J., and Daoutidis, P. (2020). Using hydrogen and ammonia for renewable energy storage: A geographically comprehensive techno-economic study. Comput. Chem. Eng. *136*, 106785.
31. Salmon, N., Bañares-Alcántara, R., and Nayak-Luke, R. (2021). Optimization of green ammonia distribution systems for intercontinental energy transport. iScience *24*, 102903.
32. Siddiqui, O., and Dincer, I. (2021). Optimization of a new renewable energy system for producing electricity, hydrogen and ammonia. Sustain. Energy Technol. Assessments *44*, 101023.
33. Sánchez, A., and Martín, M. (2018). Optimal renewable production of ammonia from water and air. J. Clean. Prod. *178*, 325–342.
34. Zhao, H., Kamp, L.M., and Lukszo, Z. (2022). The potential of green ammonia production to reduce renewable power curtailment and encourage the energy transition in China. Int. J. Hydrogen Energy *47*, 18935–18954.
35. Li, J., Lin, J., Heuser, P., Heinrichs, H., Xiao, J., Liu, F., Robinius, M., Song, Y., and Stolten, D. (2022). Co-Planning of regional wind resources-based ammonia industry and the electric network: A case study of Inner Mongolia. IEEE Trans. Power Syst. *37*, 65–80. https://ieeexplore.ieee.org/document/9471792.
36. Xu, D., Zhou, B., Wu, Q., Chung, C.Y., Li, C., Huang, S., and Chen, S. (2020). Integrated modelling and enhanced utilization of power-to-ammonia for high renewable penetrated multi-energy systems. IEEE Trans. Power Syst. *35*, 4769–4780. https://ieeexplore.ieee.org/document/9076319.
37. Allman, A., and Daoutidis, P. (2018). Optimal scheduling for wind-powered ammonia generation: Effects of key design parameters. Chem. Eng. Res. Des. *131*, 5–15.
38. Allman, A., Daoutidis, P., Tiffany, D., and Kelley, S. (2017). A framework for ammonia supply chain optimiza-tion incorporating conventional and renewable generation. AIChE J. *63*, 4390–4402.
39. Li, J., Jin, L., and Song, Y. (2020). Capacity optimization of hydrogen buffer tanks in renewable power to ammonia (P2A) system. In Proc. IEEE Power Energy Soc. Gen. Meeting, Montreal, QC, Canada, pp. 1–5. https://ieeexplore.ieee.org/document/9282084.
40. Li, J., Lin, J., Zhang, H., Song, Y., Chen, G., Ding, L., and Liang, D. (2020). Optimal investment of electrolysers and seasonal storages in hydrogen supply chains incorporated with renewable electric networks. IEEE Trans. Sustain. Energy *11*, 1773–1784. https://ieeexplore.ieee.org/document/8858041.
41. Koponen, J. (2015). Review of Water Electrolysis Technologies and Design of Renewable Hydrogen Production Systems (Lappeenranta University of Technology). https://lutpub.lut.fi/handle/10024/104326.
42. GB/T 18916.8-2017 (2017). Norm of Water Intake—Part 8：Synthetic Ammonia [S] (Beijing：Standards Press of China). https://openstd.samr.gov.cn/bzgk/gb/newGbInfo?hcno=6FF2ADA1913695C281B1F2B47C74E4EF.
43. Inner Mongolia Electric Power (Group) Co., Ltd. Announcement on power purchase price of industrial and commercial power customers in March 2023. https://www.impc.com.cn/content/202302/26/content_1004727.html.
44. Li, J., Lin, J., Song, Y., Xing, X., and Fu, C. (2019). Operation optimization of power to hydrogen and heat (P2HH) in ADN coordinated with the district heating network. IEEE Trans. Sustain. Energy *10*, 1672–1683. https://ieeexplore.ieee.org/document/8454770.
45. Inner Mongolia Autonomous Region Energy Bureau (2023). Notice on the Implementation of Renewable Energy Replacing Coal for Green Hydrogen Production Demonstration Projects. https://nyj.nmg.gov.cn/zwgk/zfxxgkzl/fdzdgknr/tzgg_16482/tz_16483/202301/t20230104_2197474.html.
46. Fan, J.-L., Yu, P., Li, K., Xu, M., and Zhang, X. (2022). A levelized cost of hydrogen (LCOH) comparison of coal-to-hydrogen with CCS and water electrolysis powered by renewable energy in China. Energy *242*, 123003.
47. Arora, P., Sharma, I., Hoadley, A., Mahajani, S., and Ganesh, A. (2018). Remote, Small-scale, 'greener ' routes of ammonia production. J. Clean. Prod. *199*, 177–192.
48. Li, G., Yang, J., Chen, D., and Hu, S. (2017). Impacts of the coming emission trading scheme on China's coal-to-materials industry in 2020. Appl. Energy *195*, 837–849.
49. China Emission Exchange (CEE) (2023). China Daily Carbon Tax. http://www.szets.com.cn/dailynewsCN/index.htm.
50. Zhang, Y., Qi, L., Lin, X., Pan, H., and Sharp, B. (2022). Synergistic effect of carbon ETS and carbon tax under China's peak emission target: A dynamic CGE analysis. Sci. Total Environ. *825*, 154076.
51. Hu, X., Wu, H., Ni, W., Wang, Q., Zhou, D., and Liu, J. (2023). Quantifying the dynamical interactions between carbon pricing and environmental protection tax in China. Energy Econ. *126*, 106912.
52. Lin, B., and Jia, Z. (2017). The impact of Emission Trading Scheme (ETS) and the choice of coverage industry in ETS: A case study in China. Appl. Energy *205*, 1512–1527.
53. Inner Mongolia Autonomous Region Energy Bureau (2022). Notice of the Energy Bureau of Inner Mongolia Autonomous Region on Printing and Distributing the Implementation of the 2022 Integrated Demonstration Project of Solar and Hydrogen Production". https://nyj.nmg.gov.cn/zwgk/zfxxgkzl/fdzdgknr/tzgg_16482/tz_16483/202209/t20220929_2143302.html.

STAR★METHODS

KEY RESOURCES TABLE

REAGENT or RESOURCE	SOURCE	IDENTIFIER
Deposited data		
Electricity price	Inner Mongolia Autonomous Region Energy Bureau	https://www.impc.com.cn/content/202302/26/content_1004727.html
Water consumption	China Standardization Administration	https://openstd.samr.gov.cn/bzgk/gb/newGbInfo?hcno = 6FF2ADA1913695C281B1F2B47C74E4EF
China daily carbon tax	China Emission Exchange	http://www.szets.com.cn/dailynewsCN/index.htm
New data generated by this study (including wind and solar power output, data used for figures)	This study	Data S1
Software and algorithms		
MATLAB	R2018b	https://www.mathworks.com/products/matlab.html
OriginLab	2021	https://www.originlab.com/

RESOURCE AVAILABILITY

Lead contact

Further information and requests for resources should be directed to and will be fulfilled by the lead author, Professor Jianxiao Wang (wang-jx@pku.edu.cn).

Materials availability

This study did not generate new unique materials.

Data and code availability

This study analyzes existing, publicly available data which are listed in the key resources table. The data generated by our analysis can be found in Data S1.

This study does not report original code, which is available for academic purposes from the lead contact.

Any additional information required to reanalyze the data reported in this paper is available from the lead contact upon request.

METHOD DETAILS

Coal-to-ammonia system

To meet the ammonia output of the existing industrial park, a reasonable configuration strategy is required for the RE2A system. This subsection provides the optimal capacity for each facility. A schematic diagram of the traditional C2A route is shown in Figure S1. The traditional process uses coal and air as raw materials, which consume electricity, water, and vapor. Starting from the air separation unit (ASU), oxygen (O_2) and nitrogen (N_2) are separated in a certain proportion. The separated O_2 is used for the gasification unit, which produces raw gas via an oxidation reaction. Then, under the influence of a catalyst and high temperature, the conversion unit produces shift gas. Through the desulfurization unit, sulfur in the shift gas is removed, generating process gas after desulfurization. Subsequently, decarbonization and hydrogen extraction occur in the pressure swing adsorption (PSA) unit to produce H_2. Through the nitrogen supplement unit, the hydrogen-nitrogen ratio of syngas is adjusted to 3:1 according to the chemical reaction in Equation 1.

$$N_2 + 3H_2 \rightleftharpoons 2NH_3, \Delta H^{o}_{298K} = -92.4 \text{ kJ/mol} \quad \text{(Equation 1)}$$

Then, a compression stage is required to compress H_2 and N_2 before feeding them into the ammonia synthesis reactor. The fresh syngas has to be treated through the Haber-Bosch process to give NH_3. Finally, liquid ammonia is separated from the mixed gas through cooling stages, which satisfies the product quality requirements.

The existing C2A system already has a mature production process, which means it does not require extra investment. Therefore, the cost model for C2A includes the costs of raw materials, operation supplies, and manpower. The cost model of C2A is given by Equation 2. The objective of the cost model is to minimize the overall production costs of the C2A system.

$$\min EX^{C2A} = EX^{MA} + EX^{C2A,EC} + EX^{MP} \quad \text{(Equation 2)}$$

$$EX^{MA} = p^{C}\sum_{t\in T} L_t^{C} \quad \text{(Equation 3)}$$

$$EX^{C2A,EC} = \sum_{t\in T} p_t^{E} P_t^{C2A,grid} + \sum_{t\in T} p^{W} L_t^{C2A,W} \quad \text{(Equation 4)}$$

where EX^{MA} represents the cost of raw materials, $EX^{C2A,EC}$ represents the operating supply costs of the C2A system, and EX^{MP} represents the cost of manpower. t and T represent the indicator of time intervals and the set of time intervals, respectively. p^C, p_t^E, and p^W represent the prices of coal, electricity and water, respectively. $P_t^{C2A,grid}$, L_t^C, and $L_t^{C2A,W}$ represent power purchased from the grid and coal and water consumption in C2A, respectively.

subject to

$$\dot{n}_t^{O_2} : \dot{n}_t^{H_2} : \dot{n}_t^{N_2} : \dot{n}_t^{NH_3} = 1.2 : 3 : 1 : 2, \forall t \quad \text{(Equation 5)}$$

$$P_t^{C2A,grid} = P_t^{C2H} + P_t^{OS} + P_t^{AS}, \forall t \quad \text{(Equation 6)}$$

$$P_t^{C2H} = \lambda \dot{n}_t^{H_2}, \forall t \quad \text{(Equation 7)}$$

$$P_t^{OS} = \varphi \dot{n}_t^{O_2} = \frac{2}{5}\varphi \dot{n}_t^{H_2}, \forall t \quad \text{(Equation 8)}$$

$$P_t^{AS} = \psi \dot{n}_t^{NH_3} = \frac{2}{3}\psi \dot{n}_t^{H_2}, \forall t \quad \text{(Equation 9)}$$

$$\mu_t^{AS} k^{AS,min} \dot{n}_t^{NH_3} \leq \dot{n}_t^{H_2} \leq \mu_t^{AS} k^{AS,max} \dot{n}_t^{NH_3}, \forall t \quad \text{(Equation 10)}$$

$$-r^{down} \dot{n}_t^{NH_3} \leq \dot{n}_{t+1}^{H_2} - \dot{n}_t^{H_2} \leq r^{up} \dot{n}_t^{NH_3}, \forall t \quad \text{(Equation 11)}$$

$$\sum_{t\in T} f^{G2L} \dot{n}_t^{NH_3} \geq \dot{n}^{NH_3}, \forall t \quad \text{(Equation 12)}$$

where $\dot{n}_t^{O_2}$, $\dot{n}_t^{H_2}$, $\dot{n}_t^{N_2}$, and $\dot{n}_t^{NH_3}$ represent the production rates of O_2, H_2, N_2, and NH_3 in C2A, respectively. P_t^{C2H}, P_t^{OS}, and P_t^{AS} represent the power consumption of coal-to-hydrogen, O_2 separation and NH_3 synthesis, respectively. λ, φ, and ψ represent the energy consumption coefficients of coal-to-hydrogen, O_2 separation and NH_3 synthesis, respectively. μ_t^{AS} is a binary variable for ammonia synthesis reactors. $k^{AS,min}$ and $k^{AS,max}$ represent the lower and upper limits of the hydrogen flow rate, respectively. r^{down} and r^{up} represent the ramp-down and ramp-up rates of the hydrogen flow rate, respectively. f^{G2L} is the coefficient of NH_3 to liquid ammonia. $\dot{n}^{NH_3}$ is the NH_3 demand in the market.

Equation 5 represents the material flow equilibrium for ammonia synthesis reactors. Equation 6 represents the limit for power balance at each moment. Equations 7, 8, and 9 represent the power consumption of coal-to-hydrogen, oxygen separation, and ammonia synthesis, respectively. Equation 10 represents the lower and upper limits of the hydrogen outflow rate due to limits in the operation temperature of the catalyst. Equation 11 represents the ramp-up and ramp-down limits for ammonia synthesis reactors. Equation 12 represents the limit for ammonia total demand.

Renewable-to-ammonia system

Based on the C2A process, a novel RE2A process is proposed by integrating H_2 from wind and solar power. Its schematic diagram is shown in Figure S2.

The new integrated process is composed of an ASU, a green hydrogen production system, a buffer and an ammonia synthesis system. With the assistance of wind and solar power, the electrolyzer converts water into H_2 and O_2. The electrochemical reaction expression is as follows:

$$H_2O \rightarrow H_2 + \frac{1}{2}O_2, \Delta H_{298K}^{o} = 285.8\ \text{kJ / mol} \quad \text{(Equation 13)}$$

After H_2 is produced, it has to be injected into the hydrogen storage tank, a bridge between the hydrogen production system and ammonia synthesis system, which adjusts the flow rate into the target range of the reactor. Then, H_2 from the hydrogen storage tank is mixed with N_2, previously obtained from ASU, to produce NH_3. The steps from gas to liquid are the same as for C2A.

From the standpoint of the power system, RE2A is modeled as a variable power load with temporal constraints on the operation security of each facility. It should be noted that the uncertainties of wind and solar power are characterized by a series of scenarios. The objective of the capacity optimization model is to minimize the total investment and operation costs of the RE2A system.

Based on the C2A system, we change the route of H_2 production to retrofit C2A into RE2A, which means that only the hydrogen-related components will be constructed while the ASU and ammonia synthesis reactor from the C2A system remain. Therefore, the investment for RE2A includes wind turbines, PV panels, electrolysers, and hydrogen buffer tanks.

$$\min EX^{\mathrm{RE2A}} = EX^{\mathrm{IN}} + EX^{\mathrm{RE2A,EC}} + EX^{\mathrm{MP}} \quad \text{(Equation 14)}$$

$$EX^{\mathrm{IN}} = \mathrm{CRF}(r,n)\left[I^{\mathrm{WP}}C^{\mathrm{WP}} + I^{\mathrm{PV}}C^{\mathrm{PV}} + I^{\mathrm{EW}}C^{\mathrm{EW}} + I^{\mathrm{HS}}C^{\mathrm{HS}}\right] \quad \text{(Equation 15)}$$

$$EX^{\mathrm{RE2A,EC}} = \sum_{t\in T}\sum_{s\in\Omega} p_t^{\mathrm{E}} p_s P_{s,t}^{\mathrm{RE2A,grid}} + \sum_{t\in T}\sum_{s\in\Omega} p^{\mathrm{W}} p_s L_{s,t}^{\mathrm{RE2A,W}} \quad \text{(Equation 16)}$$

$$\mathrm{CRF}(r,n) = \frac{r(1+r)^n}{(1+r)^n - 1} \quad \text{(Equation 17)}$$

where $EX^{\mathrm{RE2A,EC}}$ represents the operating supply costs of the RE2A system. $\mathrm{CRF}(r,n)$ is a capital recovery factor including the facility lifetime n and discount rate r. I^{WP}, I^{PV}, I^{EW}, and I^{HS} represent the initial investment of wind turbines, photovoltaic panels, electrolysers, and hydrogen buffer tanks, respectively. C^{WP}, C^{PV}, C^{EW}, and C^{HS} represent the capacity of wind turbines, photovoltaic panels, electrolysers, and hydrogen buffer tanks, respectively. s and Ω represent the indicator of a scenario and the set of scenarios, respectively. $P_{s,t}^{\mathrm{RE2A,grid}}$ and $L_{s,t}^{\mathrm{RE2A,W}}$ represent power purchased from the grid and water consumption in the RE2A system.

subject to

$$\dot{n}_{s,t}^{H_2,\mathrm{out}} : \dot{n}_{s,t}^{N_2} : \dot{n}_{s,t}^{NH_3} = 3:1:2, \forall s,t \quad \text{(Equation 18)}$$

$$P_{s,t}^{\mathrm{WP}} + P_{s,t}^{\mathrm{PV}} + P_{s,t}^{\mathrm{RE2A,grid}} = P_{s,t}^{\mathrm{EW}} + P_{s,t}^{\mathrm{NS}} + P_{s,t}^{\mathrm{AS}}, \forall s,t \quad \text{(Equation 19)}$$

$$\dot{n}_{s,t}^{H_2,\mathrm{in}} = \frac{\eta^{\mathrm{EW}} P_{s,t}^{\mathrm{EW}} \cdot 3600}{\mathrm{HHV}}, \forall s,t \quad \text{(Equation 20)}$$

$$\mu_{s,t}^{\mathrm{EW}} k^{\mathrm{EW,min}} C^{\mathrm{EW}} \le P_{s,t}^{\mathrm{EW}} \le \mu_{s,t}^{\mathrm{EW}} k^{\mathrm{EW,max}} C^{\mathrm{EW}}, \forall s,t \quad \text{(Equation 21)}$$

$$P_{s,t}^{\mathrm{NS}} = \varphi \dot{n}_{s,t}^{N_2} = \frac{1}{3}\varphi \dot{n}_{s,t}^{H_2,\mathrm{out}}, \forall s,t \quad \text{(Equation 22)}$$

$$P_{s,t}^{\mathrm{AS}} = \psi \dot{n}_{s,t}^{NH_3} = \frac{2}{3}\psi \dot{n}_{s,t}^{H_2,\mathrm{out}}, \forall s,t \quad \text{(Equation 23)}$$

$$C_{s,t+1}^{\mathrm{HS}} = C_{s,t}^{\mathrm{HS}} + \left(\eta^{\mathrm{HS}} \dot{n}_{s,t}^{H_2,\mathrm{in}} - \dot{n}_{s,t}^{H_2,\mathrm{out}} \middle/ \eta^{\mathrm{HS}}\right), \forall s,t \quad \text{(Equation 24)}$$

$$C_0^{\mathrm{HS}} = C_T^{\mathrm{HS}} \quad \text{(Equation 25)}$$

$$0 \le C_{s,t}^{\mathrm{HS}} \le C^{\mathrm{HS}}, \forall s,t \quad \text{(Equation 26)}$$

$$0 \le P_{s,t}^{\mathrm{WP}} \le \sum_{s\in\Omega} p_s P_{s,t,\max}^{\mathrm{WP}}, \forall s,t \quad \text{(Equation 27)}$$

$$0 \le P_{s,t}^{\mathrm{PV}} \le \sum_{s\in\Omega} p_s P_{s,t,\max}^{\mathrm{PV}}, \forall s,t \quad \text{(Equation 28)}$$

$$-P_{\max}^{\mathrm{grid}} \le P_{s,t}^{\mathrm{RE2A,grid}} \le P_{\max}^{\mathrm{grid}}, \forall s,t \quad \text{(Equation 29)}$$

$$\mu_{s,t}^{\mathrm{AS}} k^{\mathrm{AS,min}} \dot{n}_{s,t}^{NH_3} \le \dot{n}_{s,t}^{H_2,\mathrm{out}} \le \mu_{s,t}^{\mathrm{AS}} k^{\mathrm{AS,max}} \dot{n}_{s,t}^{NH_3}, \forall s,t \quad \text{(Equation 30)}$$

$$-r^{\mathrm{down}} \dot{n}_{s,t}^{NH_3} \le \dot{n}_{s,t+1}^{H_2,\mathrm{out}} - \dot{n}_{s,t}^{H_2,\mathrm{out}} \le r^{\mathrm{up}} \dot{n}_{s,t}^{NH_3}, \forall s,t \quad \text{(Equation 31)}$$

$$\sum_{t\in T}\sum_{s\in\Omega} f^{\mathrm{G2L}} p_s \dot{n}_{s,t}^{NH_3} \ge \dot{n}^{NH_3}, \forall s,t \quad \text{(Equation 32)}$$

where $\dot{n}_{s,t}^{H_2,in}$, $\dot{n}_{s,t}^{H_2,out}$, $\dot{n}_{s,t}^{N_2}$, and $\dot{n}_{s,t}^{NH_3}$ represent the H_2 input and output flow rates of the hydrogen storage tanks and the N_2 and NH_3 production rates in RE2A. $P_{s,t}^{WP}$ and $P_{s,t}^{PV}$ represent the generation of wind and photovoltaic power, respectively. $P_{s,t}^{EW}$, $P_{s,t}^{NS}$, and $P_{s,t}^{AS}$ represent the power consumption of water electrolysis, N_2 separation and NH_3 synthesis in RE2A, respectively. η^{EW} represents the energy conversion efficiency of the electrolysers. HHV is the higher heating value of H_2. μ_t^{EW} is a binary variable for electrolysers. $k^{EW,min}$ and $k^{EW,max}$ represent the lower and upper limits of the load power of the electrolysers, respectively. φ represents the energy consumption coefficient of N_2 separation. C_0^{HS}, $C_{s,t}^{HS}$, and C_T^{HS} represent the H_2 inventory in the storage tank at the initial time, time t, and final time, respectively. η^{HS} represents the hydrogen inflow and outflow efficiency of the hydrogen storage tanks. p_s represents the weight of scenario s. $P_{s,t,max}^{WP}$, $P_{s,t,max}^{PV}$, and P_{max}^{grid} represent the maximal power generation of wind turbines, photovoltaic panels and power purchased from the grid.

Equation 18 represents the material flow equilibrium for ammonia synthesis reactors. Equation 19 represents the limit for power balance at each moment. Equation 20 represents the energy conversion efficiency of the electrolyzer. Equation 21 represents the lower and upper limits of the electrolyzer. Equations 22 and 23 represent the power consumption of nitrogen separation and ammonia synthesis, respectively. Equations 24–26 represent the operation limits of the hydrogen buffer tanks. Equations 27, 28, and 29 represent the lower and upper limits of wind power, solar power, and power purchased from the grid, respectively. Equation 30 represents the lower and upper limits of the hydrogen outflow rate due to limits in the operation temperature of the catalyst. Equation 31 represents the ramp-up and ramp-down limits for ammonia synthesis reactors. Equation 32 represents the limit for ammonia total demand.

Data resources

The data used in the case studies are shown in Table S1 and Figure S3.